University of Szeged
Albert Szent-Györgyi Medical School
Doctoral School of Clinical Medicine

Adaptive radiotherapy in different tumor sites

PhD Thesis

Zoltán Végváry, M.D.

Supervisor(s):

Katalin Hideghéty, M.D., Ph.D., Habil

Szeged
2025

List of full papers that served as the basis of the Ph.D. thesis

I. **Végváry Z**, Darázs B, Paczona V, Dobi Á, Reisz Z, Varga Z, Fodor E, Cserháti A, Oláh J, Kis D, Barzó P, Hideghéty K. Adaptive Radiotherapy for Glioblastoma Multiforme - The Impact on Disease Outcome.
Anticancer Res. 2020 Aug;40(8):4237-4244. doi: 10.21873/anticanres.14425.
IF: 2.480

II. **Végváry Z**, Kószó R, Együd Z, Varga L, Paczona VR, Cserháti A, Gal V, Varga Z, Nagy Z, Deák B, Borzák F, Bontovics J, Fodor E, Oláh J, Kahán Z. MRI-based image-guided adaptive brachytherapy for locally advanced cervical cancer in clinical routine: a single-institution experience.
Pathol Oncol Res. 2025 May 1;31:1612077. doi: 10.3389/pore.2025.1612077.
IF: 2.300

Related articles

I. Darázs B, Ruskó L, **Végváry Z**, Ferenczi L, Dobi Á, Paczona V, Varga Z, Fodor E, Hideghéty K. Subventricular zone volumetric and dosimetric changes during postoperative brain tumor irradiation and its impact on overall survival.
Phys Med. 2019 Dec;68:35-40. doi: 10.1016/j.ejmp.2019.10.039.
IF: 2.485

II. Paczona VR, **Végváry Z**, Kelemen G, Dobi Á, Borzási E, Varga L, Cserháti A, Csomor A, Radics B, Dósa S, Balázsfi M, Fodor E, Borzák F, Puskás Á, Varga Z, Oláh J, Hideghéty K. Magnetic resonance imaging in glioblastoma radiotherapy - beyond treatment adaptation.
Phys Imaging Radiat Oncol. 2025 Mar 20;34:100754. doi:10.1016/j.phro.2025.100754.
IF: 3.400

III. **Végváry Z.**
Modern képadaptív sugárterápia a lokálisan előrehaladott méhnyakrák kuratív kezelésében.
Onkológia & Hematológia, 14 (2). pp. 94-98. ISSN 2559-8066 (2024)

Table of contents

List of abbreviations

3D	3-dimensional
AIO	All In One
ART	adaptive radiotherapy
BT	brachytherapy
CBCT	cone-beam computer tomography
CRT	chemoradiotherapy
CT	computer tomography
CTCAE	Common Terminology Criteria for Adverse Events
CTV	clinical target volume
CTVHR	high-risk clinical target volume
EANO	European Association of Neuro-Oncology
EBRT	external beam radiotherapy
eGFR	estimated glomerular filtration rate
EORTC	European Organisation for Research and Treatment of Cancer
EQD2	2Gy/fraction equivalent dose
ESTRO	European SocieTy for Radiotherapy & Oncology
FDOPA	3,4 dihydroxy 6 [18F] fluoro-L phenylalanine
FET	O-(2-[18F]fluoroethyl)-L-tyrosine
FIGO	International Federation of Gynecology and Obstetrics
FLAIR	fluid-attenuated inversion recovery
FSE	fast spin echo
GBM	glioblastoma
GEC	The Groupe Européen de Curiethérapie
GTV	gross tumor volume
GTVinit	initial gross tumor volume
GTVres	residual gross tumor volume
HD	high definition
HDR	high dose-rate

HPV	Human papillomavirus
HR	hazard ratio
IC	intracavitary
IC/IS	intracavitary/interstitial
ICRU	International Commission on Radiation Units and Measurements
IGABT	image-guided adaptive brachytherapy
IGART	image-guided adaptive radiotherapy
IMRT	intensity-modulated radiation therapy
KPS	Karnofsky Performance Status
LACC	locally advanced cervical cancer
LINAC	linear accelerator
MET	11C-methionine
MGMT	O-6 methylguanine DNA methyltransferase
MRI	magnetic resonance imaging
OAR	organ at risk
OS	overall survival
OTT	overall treatment time
PAO	para-aortic lymph node region
PD-L1	programmed death-ligand 1
PET	positron emission tomography
PFS	progression-free survival
PIBS	Posterior-Inferior Border of Symphysis
PIL	parailiac lymph node region
PTV	planning target volume
QOL	quality of life
RT	radiation therapy
RTOG	Radiation Therapy Oncology Group
SD	standard deviation
SVZ	subventricular zone
T2w	T2 weighted

1. Introduction

Adaptive radiotherapy (ART) approaches have been in the focus of research as part of radiation oncology development since the last three decades. Among numerous factors contributing to the advancement the implementation of modern image-guidance into treatment delivery has a major importance (1). Recently, image-guided ART (IGART) techniques have been widely used in different tumor sites, including glioblastoma (GBM) and locally advanced cervical cancer (LACC) as well.

The advent of various forms of high-tech volumetric imaging has opened up the possibility of defining and following target and normal structures in the brain with high resolution prior to and during a course of radiation therapy (RT). Enhanced dose-delivery methods using new generation linear accelerators (LINAC) or increasingly available nuclear particle accelerators allow highly selective dose distribution for predefined structures (2-5). These developments can lead to a remarkably improved therapeutic ratio. Toward that goal, many newly defined structures have to be delineated. Furthermore, if the volume and location of the primarily contoured structures change, particularly small structures (such as chiasma, subventricular zone (SVZ) and hippocampus), those should also be followed and the RT plan subsequently modified (6). Several studies have investigated spatial and dosimetric changes in critical structures during treatment for different cancer types (7-9), but much less research has been performed on RT of the brain, which has great anatomical constancy due to the closed skull volume and lack of organ movement. However, tumor volume, the surgical cavity, the peritumoral region and several sensitive brain structures are assumed to undergo slow but evident changes (e.g. hemorrhage, edema and shift of anatomical structures) owing to the development of radiation-related reactions and residual tumor response (10-13). The importance of such anatomical changes during the course of RT increases if growing numbers of small substructures [target and organs at risk (OARs)] are defined for dose prescription. The standard OARs for brain tumor RT include the optic nerves, optic chiasm, eyes, lenses, brain and brainstem. Optionally, the cochleae, lacrimal glands, pituitary gland, hypothalamus and hippocampus could be taken into account for treatment planning when the tumor is in a location that will allow sparing without compromising the dose to the target (14-16). Glioblastoma is a tumor that invades surrounding tissues aggressively, becomes infiltrative and spreads into different regions of the brain. Defining the clinical target volume (CTV) on postoperative images is therefore a highly

challenging task (17-19). Preoperative contrast-enhancing volume cannot be directly used due to postoperative changes, and the resection cavity does not correspond accurately to the high number tumor cell region. Additionally, residual contrast-enhancing and non-enhancing tumor should be included in the CTV. Recently, advanced imaging techniques have been recommended to define the volume of the tumor mass, such as different sequences of magnetic resonance imaging (MRI) and amino acid-based positron-emission tomography (PET) images (11C-methionine (MET), O-(2-[18F]fluoroethyl)-L-tyrosine (FET) and 3,4 dihydroxy 6 [18F] fluoro-L phenylalanine (FDOPA)) (17-21). Furthermore, different approaches to the definition of target volumes are practiced according to guidelines of different RT societies. Previously both The Radiation Therapy Oncology Group (RTOG) and the European Organisation for Research and Treatment of Cancer (EORTC) recommended a 20 mm margin expanding the gross tumor volume (GTV) to create the CTV. While RTOG guidelines suggest performing a two-phase irradiation, in Europe RT is delivered in a single phase most frequently (22, 23). Nevertheless, the most recent European SocieTy for Radiotherapy & Oncology and European Association of Neuro-Oncology (ESTRO-EANO) recommendations decreased the GTV to CTV margin to 15 mm without the inclusion of postoperative edema (21). The use of several MRI sequences at different time points, including preoperative MRI with a diffusion-weighted sequence for tractography and functional MRI, thereafter MRI within 48 hours post-surgery and a further pre-RT MRI, has recently become a standard requirement (24). These imaging strategies support ART workflows that account for dynamic anatomical and biological changes, thereby improving treatment precision and outcomes in GBM. Repeated imaging during the course of RT contributes to refining the accuracy of the planning target volume (PTV): postoperative changes, such as edema and surgical cavity evolution, tend to stabilize over time, allowing for a clearer visualization of the residual tumor. Additionally, ongoing changes in tumor size and the spatial relationships with surrounding healthy tissues can be captured and incorporated into treatment adaptation, ultimately enhancing dose conformity and sparing of critical structures. While GBM management highlights the importance of repeated imaging for ART, the need for adaptation is arguably even more pronounced in cervical cancer. This disease continues to be a significant health issue and cause of cancer morbidity and mortality, with around 660,000 new cases and 350,000 deaths related to the disease globally each year and approximately 1,000 new cases and about 400 deaths in Hungary (25). Radiotherapy, especially when using the IGART approach, plays a crucial role in improving outcomes. It is estimated that by implementing an IGART technique, 5-year disease-free survival will be more than 90% among patients with locoregional disease (26). While early-stage cervical cancer can be cured

with surgery or even with RT alone in certain clinical circumstances, the standard curative treatment for LACC is concomitant chemoradiotherapy (CRT) (27-32). Intracavitary (IC) or combined intracavitary/interstitial (IC/IS) brachytherapy (BT) has been an essential component of the IGART approach in the last decade. No relevant clinical data indicate that BT boost could be replaced by any advanced external beam radiotherapy (EBRT) technique providing an equivalent outcome (33). Due to excellent soft tissue resolution providing additional information regarding residual tumor extent, environmental propagation, and surrounding normal anatomy, MRI-based image-guided adaptive BT (IGABT) has become the gold standard curative treatment for LACC (26). Since access to MRI has been limited in many clinical centers and its shortage is often aggravated by logistical and financial obstacles, computed tomography (CT)-based 3-dimensional (3D) image guidance is often used to replace MRI for BT planning. Based on The Groupe Européen de Curiethérapie (GEC) and the European SocieTy for Radiotherapy & Oncology (ESTRO) recommendations, the widespread use of MRI-based image guidance has been receiving increasing clinical support in terms of both precision treatment planning and clinical outcome. The EMBRACE-I trial is considered to be the first prospective multicenter study offering a benchmark for the utilization of MRI-guided IGABT, with an excellent 92% overall 5-year local control rate (34). Data from retroEMBRACE, a large retrospective multicenter analysis ongoing in parallel with EMBRACE-I, showed an 89% overall local control rate at 5 years (35). Consequently, the EMBRACE-II was launched in 2016 as the first prospective multicenter interventional study aiming at uniform target concept and dose prescription protocol for MRI-guided IGABT to further improve efficiency and reduce treatment-related moderate and severe morbidity. Since MRI-guided IGABT provides individually inhomogeneous dose distribution and the possibility of dose escalation in large and irregular volumes based on complex applicator arrangements and 3D treatment planning, this sophisticated technique ensures a superior outcome reinforced by the excellent clinical results from the previous EMBRACE studies (36).

2. Aims

2.1. To evaluate and validate the institutional protocol for target volume definition in the RT of high-grade gliomas, with a focus on the integration of multimodal imaging and adaptive planning strategies.

2.2. To analyze the relationship between postoperative RT parameters - particularly GTV and PTV - and clinical outcome, overall survival (OS) in patients with high-grade gliomas.

2.3. To investigate the potential of the use of repeated CT/MRI during two-phase RT delivery and adaptation of the structure definition for replanning during postoperative/curative CRT in GBM patients and to evaluate the impact of changes on dosimetry and clinical outcomes.

2.4. To analyze our first findings on both the dosimetry and treatment-related toxicity aspects in LACC patients treated with curative CRT and IGABT boost depending on the BT technique applied (MRI based vs non-MRI based).

3. Patients and methods

All the researches conducted on ART had been approved by the Human Investigation Review Board, University of Szeged, Albert Szent-Györgyi Clinical Centre (46/2015-SZTE and 68/2015-SZTE).

3.1. Adaptive Radiotherapy for Glioblastoma Multiforme - The Impact on Disease Outcome

3.1.1. Study characteristics

Our retrospective analysis included patients diagnosed with histologically proven GBM undergoing postoperative/definitve CRT after neurosurgical intervention (biopsy or tumor resection). Patients were treated with 75 mg/m2 temozolomide each day during RT, with a 60 Gy total dose administered in two phases (40 Gy + repeated planning CT/MRI-based replanning of a 20 Gy boost) conventionally fractioned at 2 Gy per fraction. Patient and tumor specific data were obtained from case history files.

3.1.2. Contouring and treatment planning

Patients were positioned and fixed using a 3-point individual thermoplastic mask, with a CT scan taken with slice thickness of ≤5 mm with the patient in a supine position. The GTV and PTV were defined on the primary CT using pre- and postoperative MRI images. Registration and contouring were performed with Advantage SIM software (version 4.7; General Electric Healthcare, Chicago, IL, USA). Contouring was performed in axial reconstructions of the CT data set after MRI-CT image fusion. The PTV margin around the GTV on the preoperative gadolinium-enhanced T1-weighted MRI sequence was defined according to our institutional protocol based on the actual RTOG contouring guidelines (22). Around the GTV, a 20 mm margin was created encompassing the peritumoral edema defined on the basis of postoperative T2-FLAIR MRI. In the case of excessive edema, the margin was adapted manually in individual cases. All plans were made and optimized in the Xio Planning System (version 4.7; Elekta, Stockholm, Sweden). The PTV was treated with 3-dimensional conformal RT or intensity-modulated RT (IMRT) up to 40 Gy in 20 fractions with regular position control using portal imaging or cone-beam CT (CBCT). After the first period of study, a second planning CT or,

more recently, MRI was performed. GTV1 and PTV1 were defined on the secondary planning CT. When an MRI was taken, image registration was applied for delineation of GTV1 and PTV1 on the planning CT (Figure 1). PTV1 was assigned by adding a 10 mm margin around GTV1. The PTV1 volume was treated with 3D-conformal RT/IMRT delivering an additional 20 Gy in 10 fractions.

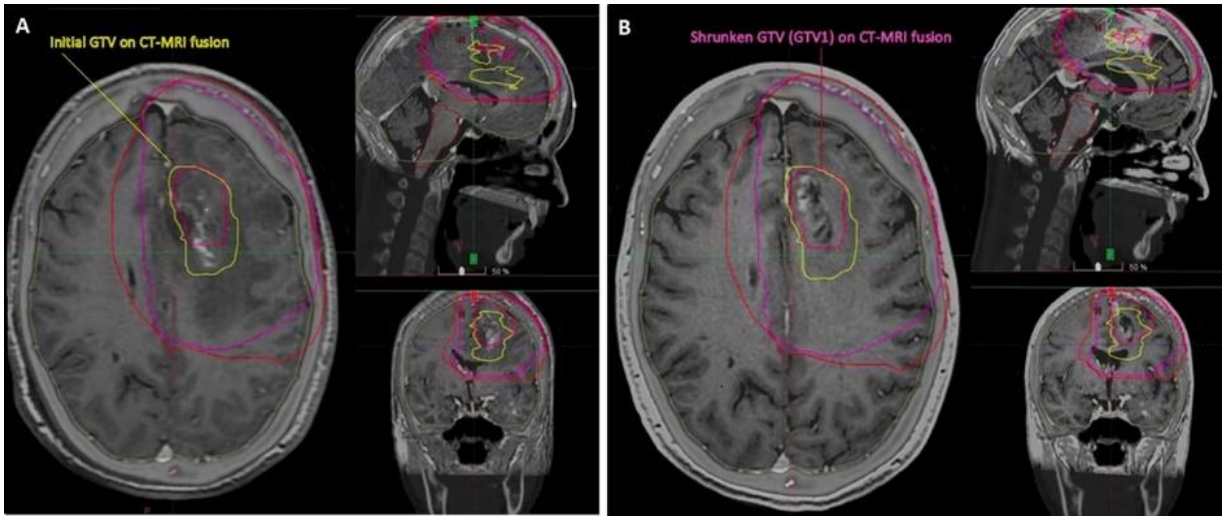

Figure 1: A: Initial gross tumor volume (GTV - yellow) and planning target volume (PTV - red) after 40 Gy. B: Irradiation target volumes were recontoured (GTV1 - pink; PTV1 - purple).

3.1.3. Statistical analysis

The primary endpoint was OS and target-volume parameters. Overall survival was measured from the date of histological diagnosis to the date of death from any cause. Patients who developed none of these time-to-event endpoints were censored on the date of their last follow-up. Survival distributions and median survival data were estimated using the Kaplan–Meier method, and comparisons were performed based on the log-rank test for categorical characteristics. Cox proportional hazards regression models were fitted to examine the association of RT parameters with OS. Variables with p-values of less than 0.05 in the univariate analysis were selected for the multivariate Cox proportional hazards model. Statistical analysis was performed using the SPSS statistical analysis software package (version 20; IBM, Armonk, NY, USA). Statistical significance was set at a threshold of $p<0.05$.

3.2. MRI-based image-guided adaptive brachytherapy for locally advanced cervical cancer in clinical routine: a single-institution experience

3.2.1. Background of study

We introduced the IGART technique in routine practice in our department at the end of 2015 for the definitive CRT of LACC patients. As a next step, we set out to introduce and adapt the recommendations of the EMBRACE-II protocol (26). For various reasons, not all patients received MRI-based IGABT during the procedure. With our retrospective study we intended to anyalyse radiotherapy-related parameters and the treatment's feasibility based on acute toxicity in two cohorts of patients comparing MRI-based IGABT versus CT only (non-MRI-based) BT boost as part of the definitive treatment for LACC.

Inclusion criteria used the stage IB-IVA International Federation of Gynecology and Obstetrics (FIGO) 2009 system and included histologically proven squamous cell carcinoma, adeno-squamous carcinoma, or adenocarcinoma of the uterine cervix and the completion of curative CRT and BT. The main exclusion criteria were the presence of distant metastases, including metastatic para-aortic lymph nodes beyond the level of the lumbal 1-2 (L1-L2) vertebral interspace, or any non-compliance to the protocol.

All patients underwent a gynecologic examination, additional cystoscopy and/or rectoscopy if organ involvement was suspected, and abdomino-pelvic MRI for pelvic staging at baseline. A diagnostic PET/CT scan was performed for the accurate assessment of lymph node involvement and exclusion of distant metastases. A second pelvic MRI was done on the fifth week of CRT in all cases to assess tumor response before the BT boost. During the MRI, contrast medium in the vagina was applied for better visualization.

3.2.2. Teletherapy technique

For EBRT, all patients went through similar treatment planning and delivery procedures. Patients were asked to empty their bowel before the treatment planning CT and each treatment session thereafter. Likewise, as a special bladder protocol, patients were instructed to urinate first, then drink 500 mL water in 30 min. Patients were positioned on the abdominal/pelvic module of the All In One (AIO) Solution (Orfit, Wijnegem, Belgium) and fixed with the Pelvicast System (Orfit, Wijnegem, Belgium). Three series of non-contrast CT scans were taken

(GE Healthcare Discovery™ RT CT, GE Healthcare, Chicago, IL, United States) from the top of the kidneys to the distal edge of the inguinal regions with an empty (0 min), comfortably filled (30 min), and full bladder (45 min).

Diagnostic T2 weighted ($T2_w$) MRI and PET/CT scans were fused to the treatment planning CT for better target definition. The delineation of the volumes of interest was based on the guidelines of the EMBRACE-II study (26, 36). Two experienced radiologists (A.C. and V.G.) participated in the contouring procedures throughout the entire RT course. Dose prescription to these target volumes and the dose constraints of the indicated OARs are presented in Table 1**.** Cumulative EBRT + IGABT 2Gy/fraction equivalent dose (EQD2) was calculated with the linear quadratic model using $\alpha/\beta = 10$ for target volumes and $\alpha/\beta = 3$ value for OARs (37). A total dose of 45 Gy was delivered to the PTV in 1.8 Gy/fraction daily doses. A simultaneously integrated boost (SIB) dose was applied to pathological lymph nodes to a total dose of 55 Gy if the parailiac lymph node region (PIL) was affected and 57.5 Gy if the para-aortic lymph node region (PAO) was affected. For dose reporting, the usual dose-volume data were utilized as indicated.

Structure	Dose prescription/dose constraint
ITV45	D99.9>42,75Gy
PTV45	D95>42,75Gy
CTV-N	D98>55Gy Dmax<58,85Gy
PTV-N	D98>49,5Gy
Bowel	V30Gy<500cm3 V40Gy<250cm3 Dmax<47.25Gy
Sigmoid	Dmax<47.25Gy
Bladder	V30Gy<80% V40Gy<60% Dmax<47.25Gy
Rectum	V30Gy<95% V40Gy<75% Dmax<47.25Gy
Femoral head	Dmax<50Gy
Body	V43Gy/VPTV45Gy<1.15

Table 1: Institutional dose prescription and dose constraints for EBRT applied

Radiation therapy was delivered with a comfortably filled bladder according to the bladder protocol. In all cases, a 5-field or 7-field inverse IMRT planning technique was applied using the Eclipse v13.6 planning system (Varian Oncology Systems, Palo Alto, CA, United States). Treatment was delivered with a Varian TrueBeamSTx or VitalBeam (Varian Oncology Systems, Palo Alto, CA, United States) linear accelerator equipped with high-definition (HD) 120 or Millenium120 multileaf collimator performing daily CBCT verification and couch repositioning referring to bony anatomy.

3.2.3. Concomitant chemotherapy

A total of five cycles of concomitant 40 mg/m^2 cisplatin per week chemotherapy was delivered during the EBRT. Possible dose reduction or withholding was based on continuous monitoring

of blood cells and kidney function using the calculation of estimated glomerular filtration rate (eGFR) (Cockcroft-Gault formula).

3.2.4. Brachytherapy technique

Following CRT, patients had three or four BT boost treatments, based on the cumulative target doses in the various target volumes and OAR dose constraints. If the risk of overlapping the hard dose constraint of the OAR at the fourth BT session was foreseen, the BT boost dose was delivered in three sessions only. The delivery of two fractions on consecutive days and another two fractions a week later was aimed at in order to complete the RT procedure within 50 days.

Before the BT session patients received an enema. A Foley catheter was inserted into the bladder and the bladder was filled with 50–100 mL of physiological saline. The volume was maintained during treatment to ensure reproducibility. In case of IC treatment, minor opiate tramadolor and muscle relaxant premedication were applied 20 min before application. For the IC/IS procedure, patients were provided epidural analgesia during the intervention, which was maintained if the applicators and the needles remained in the patient for the consecutive BT session the next day.

IC/IS BT was applied only in the MRI-based IGABT group if significant residual tumor volume or parametrial infiltration was present at the time of the BT. In the non-MRI-based BT cohort, patients were treated with the simple IC technique. CT- and MRI-compatible Ring or 3D Interstitial Ring Applicator sets (Varian Oncology Systems, Palo Alto, CA, United States) were used for all patients.

The maintenance of the geometry of the applicator towards the target volume was ensured by a tight vaginal packing aimed at pushing away the rectum and bladder and fixing the applicator against the cervix. The packing was filled with ultrasound gel to make it distinguishable from the vagina at planning. The applicator was also fixed with bandages to the patient. A special CT/MR-compatible stretcher (Spinal board BAR025, Fazzini, Italy) was used for patient transportation. The patient stayed on that device in a comfortable supine position throughout the procedure including verification and dose delivery.

After inserting the applicator(s) in all cases, a non-contrast CT series with 2.5 mm slice thickness was acquired for safety reasons and to check the applicator's position. CT verification was used before BT delivery for safety, quality assurance, and planning purposes even if an

MRI was not performed. Patients receiving MRI-based individualized IGABT were then transferred with the applicator *in situ* to the MRI unit before the first and third BT sessions at a minimum. In a few cases, $T2_w$ fast spin echo (FSE) sequences were acquired with parallel orientation regarding the cervix uteri, with 1 mm slice thickness and without an interslice gap according to the Gyn GEC ESTRO MRI guidelines (38). Thereafter, 3D $T2_w$ sequences were established for MRI-based applicator reconstruction and delineation. CT and MRI images were fused with rigid registration of soft tissues for quality control and planning purposes. Adaptive target volume definition and treatment planning objectives were performed in accordance with the International Commission on Radiation Units and Measurements (ICRU) 89 recommendations (39). The following BT target and OAR volumes were segmented: residual GTV (GTVres), high-risk CTV (CTVHR), bowel, bladder, sigmoid and rectum. For dose recording, right and left Point A were indicated. Patients were prescribed cumulative doses; the dose constraints for the OARs are indicated in Table 2. CTVHR and GVTres and OARs were delineated in an applicator *in situ* T2w MRI sequence. The latest treatment planning MRI was reused for contouring with superimposition if the succeeding second and/or fourth BT fraction was CT-based only.

Dose-volume parameter	**Prescribed dose (EQD2 α/β= 10 Gy)**	**Dose constraint (EQD2, α/β= 3Gy)**
D90 CTVHR	> 85Gy	
D98 CTVHR	> 75Gy	
D98 GTVres*	> 90Gy	
Dose to Point A, left	to be recorded	
Dose to Point A, right	to be recorded	
DBowel 2cm3		< 75Gy
DBladder 2cm3		< 85Gy
DRectum 2 cm3		< 75Gy
DSigmoid 2 cm3		< 75Gy

Table 2: Cumulative doses aimed at during IGABT (*in MRI-based IGABT only)

In the non-MRI based BT group, non-contrast CT scans were used for delineation and previous (pre-radiotherapy and pre-BT) MRI images assisted contouring. CTVHR and OARs were delineated with adaptation to the GYN GEC-ESTRO guidelines, however, no GTVres was contoured. MRI images acquired during the fifth week of EBRT helped target definition without performing CT-MRI fusion.

The BrachyVision TPS v13.6 planning system (Varian Oncology Systems, Palo Alto, CA, United States) was utilized for treatment planning. During optimization, first the built-in automatic option of the planning system was used, and then, taking into account the unique anatomical conditions, the plan was manually refined in accordance with the dosimetric goals. All patients were treated with a Varian Gammamed Plus iX (Varian Oncology Systems, Palo Alto, CA, United States) high dose-rate (HDR) afterloader.

3.2.5. Toxicity registration

Treatment-related acute morbidity was registered on a weekly basis according to the Common Terminology Criteria for Adverse Events (CTCAE v. 4.0). Clinical data on treatment-related acute skin, gastro-intestinal, genito-urinary, or hematologic toxicity and kidney function impairment was collected, and the worst toxicity grade within a category was counted in each case.

3.2.6. MRI-based quantitative tumor regression evaluation

Based on the T2w MR image series, a quantitative tumor regression analysis was performed for the MRI-based IGABT cohort during the treatment process. The initial GTV (GTVinit) was evaluated in the first diagnostic MRI while the GTVres volumes were assessed in both the pre-BT MRI and subsequent applicator *in situ* MRI sequences (Figures 2, 3).

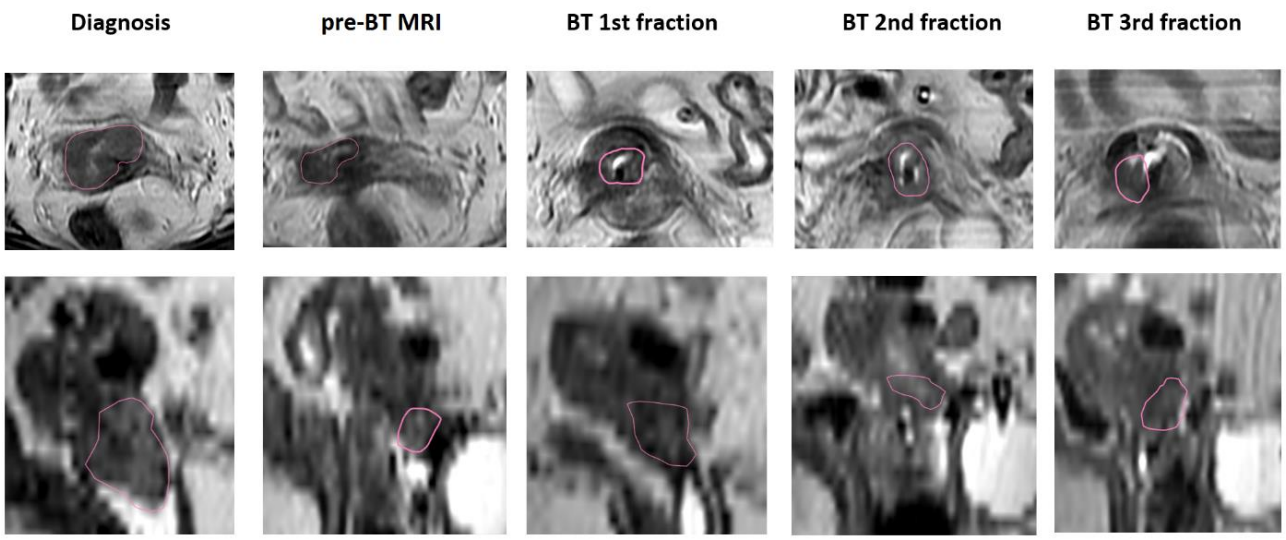

Figure 2: MRI-based GTV evaluation during treatment, transversal and sagittal views (red contour indicates the GTV)

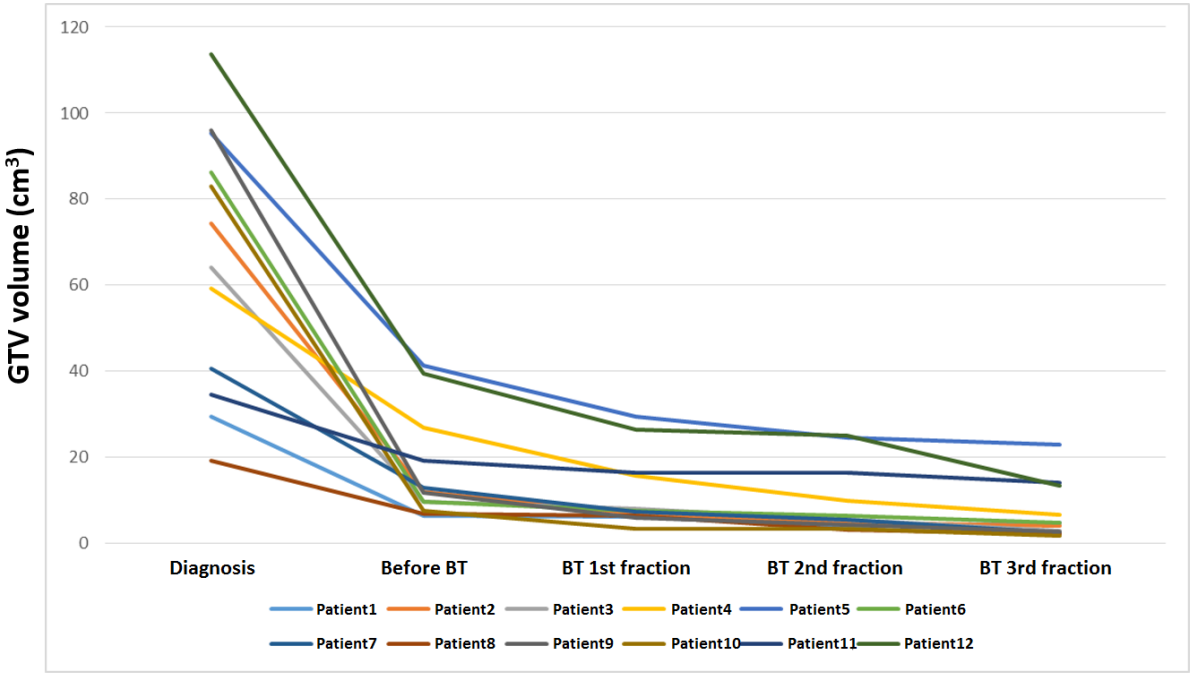

Figure 3: Quantitative MRI-based tumor regression analysis during treatment (n=12)

3.2.7. Statistical analysis

Continuous data were expressed as mean ± standard deviation (SD) values if appropriate. Tumor characteristics in the two cohorts were compared with an independent sample t-test for the continuous and Chi-squared test for the categorical variables. An independent sample t-test was used to analyze the various dose parameters between the treatment groups. Statistical software IBM SPSS statistics version 26.0 (SPSS Inc., Chicago, IL, United States) was used for statistical analysis. P-values <0.05 were regarded as statistically significant.

4. Results

4.1. Adaptive Radiotherapy for Glioblastoma Multiforme - The Impact on Disease Outcome

Forty-three consecutive patients with GBM treated at the Department of Oncotherapy University of Szeged, Hungary, between January 2013 and June 2016 were selected for a retrospective study. The patient and tumor characteristics as well as the volumetric data for the defined targets are provided in Tables 3 and 4. The average age of the 43 patients (19 males and 24 females) was 58.6 (range=12-85) years. Thirty-nine patients were treated with concurrent temozolomide chemotherapy during RT followed by temozolomide monotherapy, and four patients received only RT. All the patients underwent surgical tumor removal, with the tumor type confirmed by histology. The extent of the tumor removal of the entire study group was by subtotal resection in the majority of cases (N=27). The O-6 methylguanine DNA methyltransferase (MGMT) status was available for 33/43 tumor samples for the present analysis and 17 were defined as being promoter region methylated by immunohistochemistry. The average time to planning CT after surgery was 2.8 (range=0.7-5.1) weeks. RT generally started 1 week after the planning CT, thus the mean time interval between surgery and CRT was 29.1 (range=5-59) days. All the patients had an additional (secondary) replanning CT/MRI (mean=3.9, range=3.7-4.0 weeks) after the start of RT [mean=7.7 (range=5.3-14.3) weeks after surgery], which was registered to the initial (primary) planning CT.

Characteristic	Frequency, n
Gender	
Male	19
Female	24
Age	
≥ 60 Years	22
< 60 Years	21
Histology	
Glioblastoma	43
Type of surgery	
Biopsy	7
Subtotal resection	27
Gross total resection	9
KPS	
> 60%	16
≤ 60%	27
MGMT status	
> 40%	17
≤ 40%	16
Unknown	10
RT start	
< 27 Days	22
≥ 27 Days	21
Therapy	
Chemoradiotherapy	39
Radiotherapy alone	4

KPS: Karnofsky Performance Status; MGMT: 0-6 methylhuanine DNA methyltransferase promoter methylation; RT start: time interval between the surgery and the radiotherapy start date

Table 3: Patient and tumor characteristics

Volume	**GTV** (cm^3)	**GTV1** (cm^3)	**ΔGTV** (cm^3)	**PTV** (cm^3)	**PTV1** (cm^3)	**ΔPTV** (cm^3)
Overall	98.9±67.4	106.3±67.7	6.7±2.7	530.2±160.5	359.9±125.2	-183.2±130.5
Regression	113.1±69.4	85.5±56.9	-27.6±20.8	547.2±162.3	353.6±122.8	-193.6±124.4
No change/ progression	94.6±66.2	113.5±75.5	19.2±1.8	460.0±114.5	489.6±140.6	29.6±26.0

ΔGTV=GTV1-GTV; ΔPTV=PTV1-PTV

Table 4: Gross tumor volume (GTV) and planning target volume (PTV) on primary and on secondary (GTV1 and PTV1) computed tomography and their difference. Data are the mean±standard deviation.

The initial size of the GTV was strongly inversely correlated with OS. The patients were separated for the Kaplan–Meier analysis into two groups according to the mean GTV size: ≤99 cm3 and >99 cm3. The median OS was 25.33 months (95% CI=19.59-35.27 months) for the first group and 15.21 months (95% CI=10.82-22.27 months) for the second, corresponding to a hazard ratio (HR) of 1.006 (95% CI=1.00-1.01, p=0.031) (Figure 4A). Using the average value as cut-off point, the PTV did not exhibit a correlation with survival. Median OS was 15.21 months (95% CI=15.06-31.34 months) in the first group and 19.12 months (95% CI=15.64-28.67 months) in the second group corresponding to an HR of 1.001 (95% CI=0.99-1.01, p=0.910) (Figure 4B).

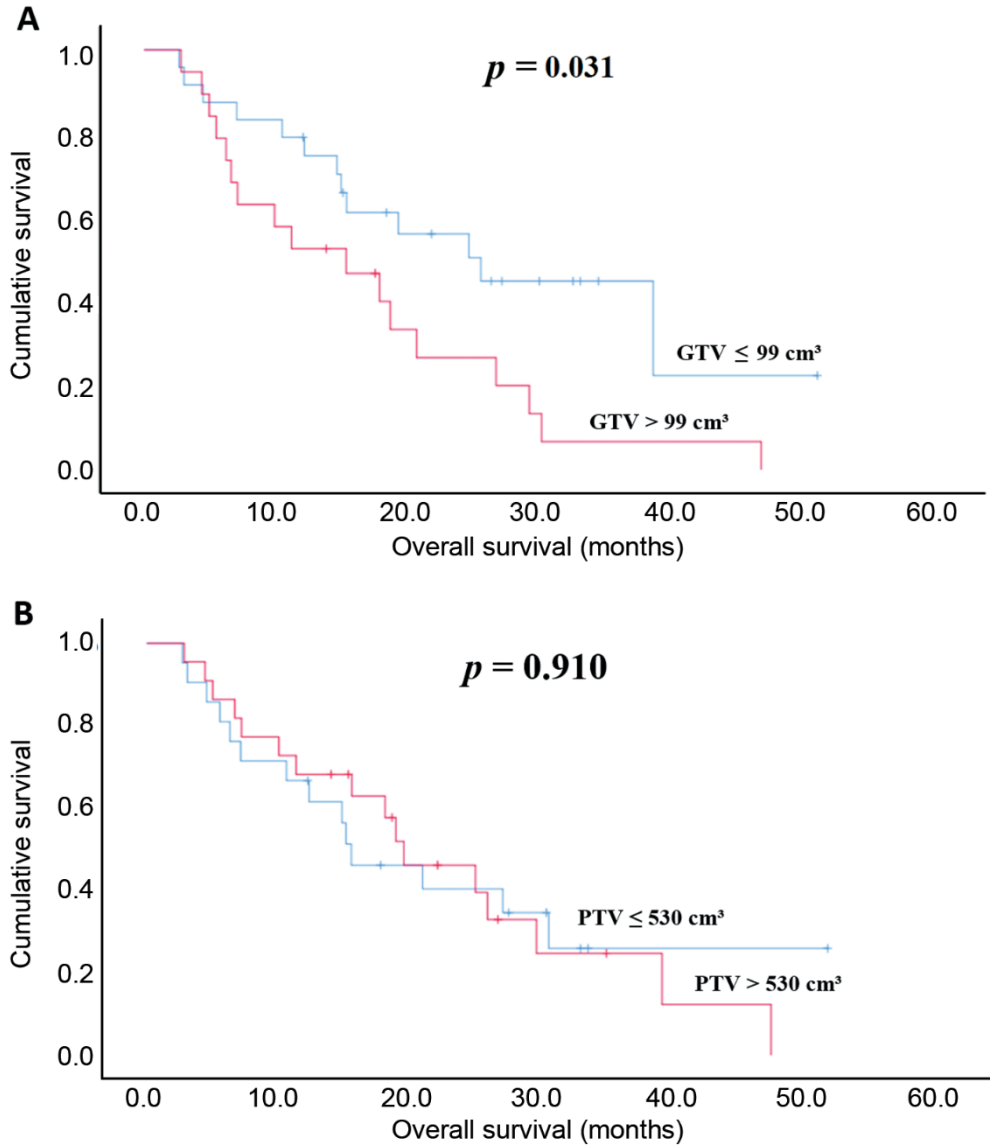

Figure 4: Correlation of change in gross tumor volume (ΔGTV) (A) and in planning target volume (ΔPTV) (B) with overall survival.

Anatomical changes in the brain and tumor growth or shrinkage occurred during RT. The GTV volume change (ΔGTV=GTV1−GTV) during RT was correlated with OS. The median OS was 25.33 months (95% CI=21.68-35.28 months) in the group with ΔGTV<0 cm3, i.e. GTV regression, and 11.10 months (95% CI=10.63-22.69 months) in the group with ΔGTV≥0 cm3, i.e. no change or progression of GTV, corresponding to an HR of 1.006 (95% CI=0.99-1.01, p=0.040) (Figure 5A). The recontouring and change of PTV was significantly different between the two groups: Patients with ΔPTV≤183 cm3 and those with ΔPTV>183 cm3. The median OS was 12.06 months (95% CI=11.63-22.91 months) for the first group and 28.98 months (95% CI=22.36-38.82 months) for the second, corresponding to an HR of 1.001 (95% CI=0.99-1.01, p=0.026) (Figure 5B).

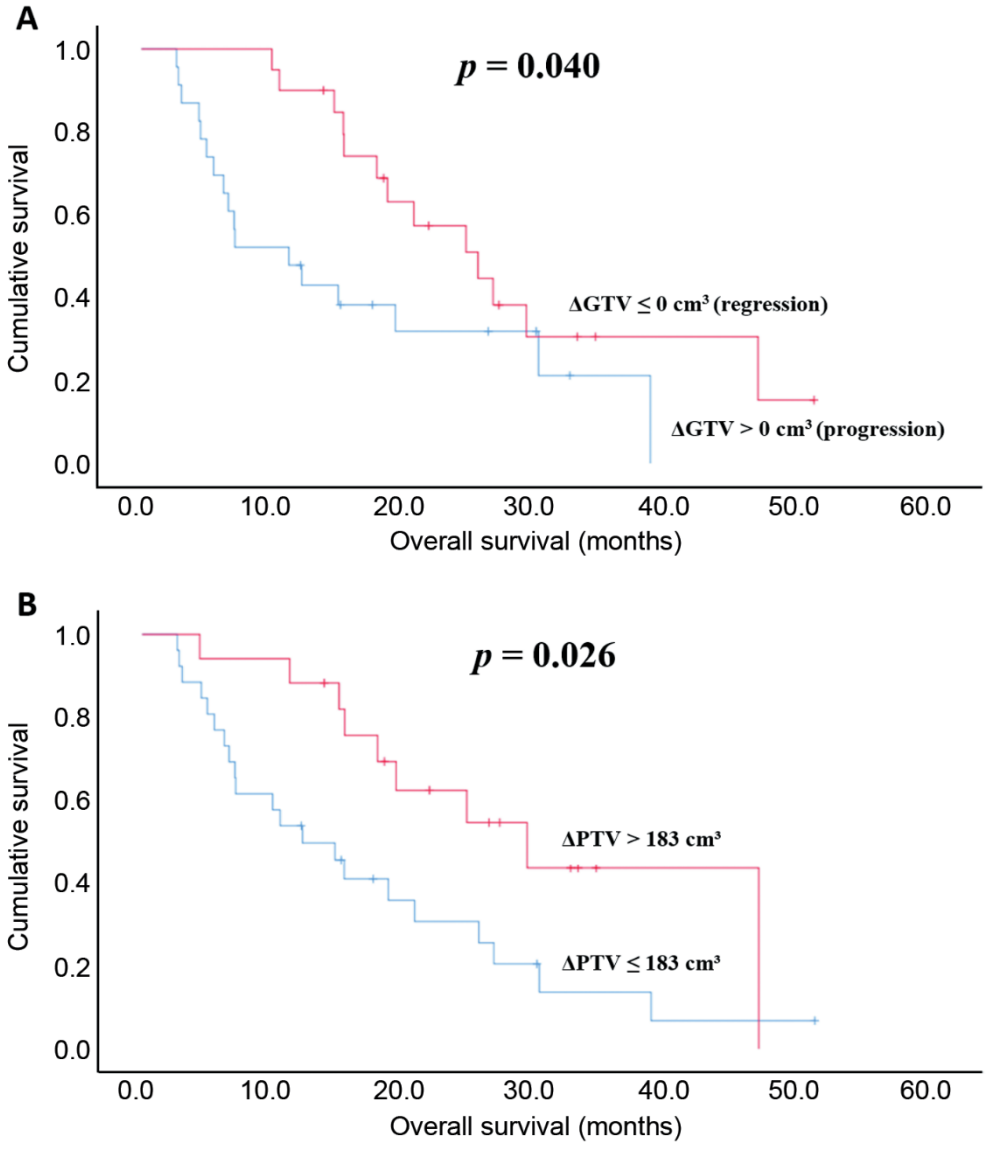

Figure 5: Correlation of change in gross tumor volume (ΔGTV) (A) and in planning target volume (ΔPTV) (B) with overall survival.

The type of surgery had a significant impact on survival, patients who underwent biopsy had a mean survival of 6.97 months, those with subtotal tumor resection 20.5 months and with gross tumor resection of 25.33 months (p=0.009) respectively. A Kaplan–Meier analysis of the time from surgery to the start of CRT and OS revealed that CRT started within 27 days resulted in a significantly higher mean OS (26.48 vs. 15.21 months, p=0.046). Our results demonstrated that MGMT promoter methylation was associated with significantly longer OS. The median OS was 7.03 (95% CI=7.58-18.44) months in those with non-methylated MGMT promoter (≤40%) and 26.48 (95% CI=19.54-35.86) months in those with>40% MGMT promoter methylation, corresponding to an HR of 1.017 (95% CI=0.99-1.03, p=0.027), retrospectively. Patients with higher postoperative KPS status (KPS>60%) also demonstrated increased OS, with 38.31 (95% CI=27.46-42.01) months versus 11.10 (95% CI=10.11-17.75) months for the other group, corresponding to an HR of 0.949 (95% CI=0.92-0.97, p<0.001).

4.2. MRI-based image-guided adaptive brachytherapy for locally advanced cervical cancer in clinical routine: a single-institution experience

The clinical data of 50 LACC patients treated with definitive CRT and IGABT boost between February 2016 and August 2022 at the Department of Oncotherapy University of Szeged were evaluated in our retrospective study. The average (±SD) age of the patients overall was 52.7 ± 12.6 years, ranging between 26 and 83 years. The median (±SD) overall treatment time was 53.8 ± 9.9 (range: 42–81) days. All patients had FIGO IB-IIIB stage LACC, 22 (44.0%) of them had negative lymph node status, and 28 (56.0%) were diagnosed with N1 disease (Table 5). The vast majority of cases, 43 patients (86.0%), had squamous cell carcinoma, while seven patients (14.0%) had adenocarcinoma. Two-thirds of the study population was diagnosed with grade 2-3 tumors (Table 5). Of the 50 patients, 43 (86.0%) completed the scheduled five chemotherapy cycles, while seven (14.0%) received only four cycles of cisplatin. In the MRI-based IGABT group, among 24 patients, eight received combined the IC/IS IGABT treatment. Altogether, six patients had three BT sessions only due to dose limitations to the OARs: one in the MRI-based IGABT group and five in the CT-based treatment group. Histology, tumor grade, FIGO, and lymph node stage were well balanced between the two treatment groups. Relevant tumor characteristics at the time of EBRT are presented in Table 5.

The features of the target volumes did not differ between the two groups; using the same EBRT technique, no significant difference was found between the coverage of PTV45, PTV-N, CTV-N_PIL, or CTV-N_PAO of the two groups, as shown in Table 6.

		MRI-based IGABT	non-MRI based IGABT	p
Stage	cT1b	4	3	0.447
	cT2a	2	4	
	cT2b	17	15	
	cT3b	1	4	
	cN0	10	12	0.783
	cN1	14	14	
	FIGO			0.293
	Ib	6	3	
	IIa	1	4	
	IIb	16	16	
	IIIb	1	3	
Pathology	Histology			0.420
	Squamos cell carcinoma	22	21	
	Adenocarcinoma	2	5	
	Grade			0.856
	I	2	3	
	II	11	10	
	III	6	5	
	NA	5	8	
Teletherapy features	GTVinit (cm3), mean±SD, range	86.02±49.68, 3.1-176.7	99.40±43.50, 43.9-192.3	0.310
	GTV-N (n=13 in both groups, cm3), mean±SD, range	8.63±6.81, 1.3-22.4	6.88±5.64, 2.1-19.9	0.483
	PTV45 (cm3) mean±SD, range	1335.0±187.1, 1083.4-1791.3	1435.9±216.6, 1123.1-1894.0	0.086
	PTVN (n=13 in both groups, cm3) mean±SD, range	63.46±63.43, 15.9-193.6	45.05±25.21, 15.1-109.3	0.363
	Small pelvis (n, %)	0, 0%	0, 0%	0.751
	Large pelvis (n, %)	17, 70.8%	20, 76.9%	
	Large pelvis+PAO (n, %)	7, 29.2%	6, 23.1%	
Chemotherapy	Number of cycles, mean±SD, range	4.88±0.32, 4-5	4.85±0.37, 4-5	0.775

Table 5: Characteristics of cases (stage, pathology, teletherapy and chemotherapy)

		MRI-based BT	non-MRI based BT	p
PTV45	V95 (%)	95.6±2.3	95.7±1.4	0.791
	Dmax (Gy)	55.4±12.6	52.5±5.6	0.275
PTVN	D98 (%)	91.0±11.3	97.1±3.0	0.187
	Dmax (Gy)	57.8±1.6	56.7±3.7	0.387
CTVN_PIL	D98 (Gy)	55.0±2.3	55.0±1.6	0.975
CTVN_PAO	D98 (Gy)	44.9±2.8	43.8±0.7	0.181

Table 6: Delivered doses to target volumes during teletherapy

While the CTVHR volumes were similar, the D90 dose to them at BT was significantly higher in the MRI-based IGABT group than in the non-MRI-based group; the CTVHR D98 doses showed a strong trend in favor of the MRI-based technique (Tables 7, 8). Likewise, the cumulative doses to the CTVHR by means of both D90 and D98 were significantly higher in the MRI-based treatment group than in the other group (Table 9). The Point A target doses, however, did not differ between the two groups (Table 8). In the MRI-based IGABT group, an average EQD2 D98 dose of 8.01 ± 1.15 (5.3–10.2) Gy per BT session and 90.08 ± 11.99 Gy cumulative dose was delivered to the GTVres (Tables 8, 9). When the doses to the CTVHR and GTVres within the MRI-based IGABT group were compared according to the BT technique, no difference was found between the IC only and IC/IS cases.

	MRI-based BT (mean±SD), range	non-MRI based BT (mean±SD), range	p
CTVHR (cm3)	28.91±11.49, 14.3-64.8	34.36±12.97, 14.8-73.5	0.123
GTVres (cm3)	6.76±5.41, 1.1-22.2	NA	NA

Table 7: Target volumes during brachytherapy

	MRI-based BT (mean±SD), range	non-MRI based BT (mean±SD), range	p
D90 CTVHR (Gy)	7.37±0.55, 5.7-8.3	6.87±0.84, 5.0-7.8	0.015
D98 CTVHR (Gy)	6.16±0.59, 4.8-7.0	5.72±0.95, 3.6-6.8	0.051
D98 GTVres (Gy)	8.01±1.15, 5.3-10.2	NA	NA
Point A left (Gy)	5.82±1.19, 3.7-9.3	5.71±0.91, 4.2-8.5	0.716
Point A right (Gy)	5.54±1.14, 3.8-8.5	5.44±0.74, 4.3-6.6	0.714

Table 8: Delivered doses to target volumes or reference points during the brachytherapy sessions

	MRI-based BT (mean±SD), range	non-MRI based BT (mean±SD), range	p
D90 CTVHR (Gy)	86.64±4.76, 74.00-95.09	81.56±8.29, 64.08-90.74	0.011
D98 CTVHR (Gy)	77.23±4.39, 67.85-84.03	73.40±7.80, 58.30-82.53	0.037
D98 GTVres (Gy)	90.08±11.99, 71.59-113.12	NA	NA

Table 9: Delivered cumulative doses to target volumes during teletherapy plus brachytherapy (EQD2, α/β=10)

Next, the same dosimetry parameters of the MRI-based IGABT cohort were studied in chronological order; an apparent increase of doses by time was found (Figure 6). The prespecified OAR doses (the EQD2 doses to 0.1 cm^3 and 2.0 cm^3 volumes of the bladder, rectum, sigmoid, and bowel) are demonstrated in Tables 10, 11. The doses to the bladder, rectum, and sigmoid did not differ between the two groups. Interestingly, significantly less dose to the bowel was experienced in Group 2, both if the dose per BT fraction and the cumulative dose after EBRT and BT was considered (Tables 10, 11). OAR doses in the MR-based IGABT cohort did not fluctuate over time.

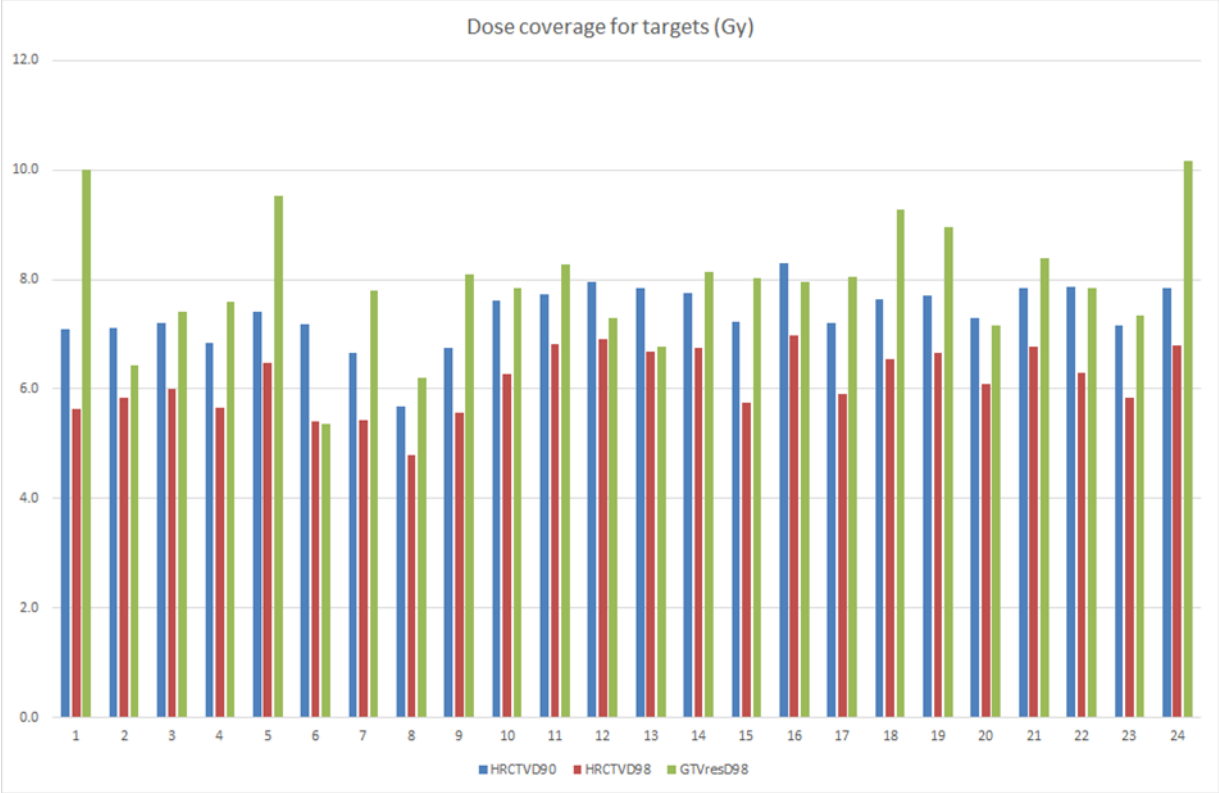

Figure 6: Individual target volume dose coverage in the MRI-based IGABT group (n=24)

	D0.1cm3 (Gy), mean±SD, range			D2cm3 (Gy), mean±SD, range		
	MRI-based BT	**non-MRI based BT**	**p**	**MRI-based BT**	**non-MRI based BT**	**p**
Bladder	7.49±.1.20, 4.5-9.4	8.10±1.24, 6.4-12.8	0.084	5.52±0.97, 2.8-6.4	5.74±0.72, 4.5-7.6	0.373
Rectum	5.61±1.41, 2.4-8.2	6.04±1.94, 2.0-9.5	0.379	3.86±0.89, 1.7-5.0	4.03±1.23, 1.5-5.9	0.597
Sigmoid	5.61±1.21, 3.7-8.9	5.48±2.02, 0.0-9.5	0.785	3.83±0.68, 2.7-5.0	3.75±1.29, 0.0-5.9	0.793
Bowel	5.34±2.27, 0.0-8.3	3.65±2.62, 0.0-7.4	0.019	3.73±1.56, 0.0-5.3	2.52±1.82, 0.0-5.0	0.015

Table 10: Dose exposure to the various OARs at single brachytherapy sessions

	D0.1cm3 (Gy), mean±SD, range			D2cm3 (Gy), mean±SD, range		
	MRI-based BT	**non-MRI based BT**	**p**	**MRI-based BT**	**non-MRI based BT**	**p**
Bladder	107.30±.17.19, 68.00-136.9	112.08±16.08, 86.17-167.3	0.315	81.53±10.07, 56.58-91.32	81.63±7.22, 63.94-92.57	0.968
Rectum	85.32±16.88, 53.87-118.14	87.13±18.78, 51.04-125.32	0.722	65.22±7.57, 49.41-75.31	66.07±8.79, 48.73-80.59	0.715
Sigmoid	83.33±14.36, 63.40-127.93	81.74±19.55, 43.20-129.35	0.746	64.64±5.66, 55.86-75.67	63.86±9.06, 43.20-76.51	0.720
Bowel	83.92±20.08, 43.20-120.45	69.23±21.19, 43.2-105.38	0.015	65.72±10.49, 43.20-78.31	57.36±11.51, 43.20-74.95	0.010

Table 11: Delivered cumulative doses to OARs during the entire course of teletherapy plus brachytherapy (EQD2, $\alpha/\beta=3$)

Regarding treatment-related side effects, the most frequent acute toxicity of any grade was nausea, leucopenia, and neutropenia in both groups. Interestingly, thrombocytopenia of grade 1 occurred significantly more in Group 2 (Table 12). There were no serious grade 3–4 adverse events registered (Table 12). No cessation of the curative treatment course was necessary due to severe toxicity.

	MRI-based BT (n=24) (%)			**non-MRI based BT (n=26) (%)**			**p**
	Grade I	**Grade II**	**Grade III**	**Grade I**	**Grade II**	**Grade III**	
Leucopenia	4 (16.7%)	11 (45.8%)	4 (16.7%)	7 (26.9%)	11 (42.3%)	1 (3.8%)	0,411
Neutropenia	3 (12.5%)	9 (37.5%)	1 (4.2%)	6 (23.1%)	4 (15.4%)	1 (3.8%)	0,325
Anaemia	9 (37.5%)	7 (29.2%)	0 (0%)	14 (53.8%)	5 (19.2%)	0 (0%)	0,494
Thrombocytopenia	6 (25.0%)	3 (12.5%)	0 (0%)	18 (69.2%)	0 (0%)	0 (0%)	0,040
Nausea	19 (79.2%)	0 (0%)	0 (0%)	13 (50.0%)	4 (15.4%)	1 (3.8%)	0,081
Vomitus	11 (45.8%)	1 (4.2%)	0 (0%)	9 (34.6%)	2 (7.7%)	0 (0%)	0,674
Enteritis	10 (41.7%)	0 (0%)	0 (0%)	13 (50.0%)	4 (15.4%)	0 (0%)	0,067
Proctitis	1 (4.2%)	0 (0%)	0 (0%)	2 (7.7%)	0 (0%)	0 (0%)	0,969
Cystitis	3 (12.4%)	1 (4.2%)	0 (0%)	1 (3.8%)	1 (3.8%)	0 (0%)	0,526
Incontinency	0 (0%)	0 (0%)	0 (0%)	0 (0%)	0 (0%)	0 (0%)	NA
Vaginitis	0 (0%)	0 (0%)	0 (0%)	2 (7.7%)	0 (0%)	0 (0%)	0,491
Dermatitis	0 (0%)	0 (0%)	0 (0%)	1 (3.8%)	0 (0%)	0 (0%)	0,978
Nephrotoxicity	3 (12.4%)	0 (0%)	0 (0%)	4 (15.4%)	0 (0%)	0 (0%)	0,875

Table 12: Treatment-induced acute toxicity (CTCAE v. 4.0)

5. Discussion

5.1. Adaptive Radiotherapy for Glioblastoma Multiforme - The Impact on Disease Outcome

In accordance with the literature, our data confirm the impact of general prognostic factors on disease outcome, *i.e.* better KPS, larger extent of tumor removal and methylated MGMT promoter status resulted in longer survival. The optimal time interval between the surgery and start of CRT is a matter of debate in the literature (40) and a clear conclusion cannot be drawn in our patient group, although the shorter time to CRT proved to be significant factor for better OS. Adaptive RT has mainly been applied in patients with extra-cranial localization taking into account anatomical changes associated with weight loss, internal organ movement, organ filling, tissue edema and potential tumor regression. These changes may significantly influence the dose distribution, resulting in target volume missing or overdosing in the OAR region. The studies published on ART have varied between daily onboard imaging-based plan adaptation and CT/MRI-based replanning prior to boost definition. The final definition of the optimal time point and methodology for these resource-consuming procedures is yet to be determined. The advantageous effect of replanning for brain irradiation is not yet supported by strong clinical evidence despite the increased attention to adaptive techniques and a growing amount of clinical data for tumors in other locations. There are limited data available on ART including brain structures in publications on head and neck region RT. A study by Ho's team found no relevant effect of a daily assessment of dose-distribution changes for the brainstem and spinal cord in oropharyngeal cancer and hence did not recommend frequent replanning from this aspect (41). In contrast, numerous other studies have confirmed the benefit of ART for the treatment of head and neck tumors to outcomes (42-46). A recent study on ART of advanced head and neck cancer demonstrated an improved therapeutic index by increasing the tumor coverage and dose reduction to the OARs (46). It confirmed that without replanning, the dose to some OARs would have exceeded their respective tolerance threshold, including central nervous system structures, *i.e.* the brainstem and spinal cord.

Unlike extra-cranial localizations, data on ART for brain tumors is sparse in spite of the fact that GBM is known as a rapidly growing tumor type, and CRT is applied postoperatively when relevant changes in post-surgical and tumor volume are supposed to occur (6, 10-13, 47). Both internationally applied guidelines (RTOG and EORTC) define target volume based on surgical cavity, edema and residual tumor. However, neither of them contains a recommendation for CT/MRI-based replanning during the course of RT. According to the institutional strategy at our Oncotherapy Department, two-phase irradiation is planned with the shrinking-volume technique. A pre-therapeutic boost definition is applied in conjunction with a recontouring of the residual tumor mass (GTV2) for repeated planning CT/MRI in an adapted CTV2-PTV2 approach. Recently, an evaluation on inter-fractional variation for completely resected GBM has been reported. Surgical cavities of 19 patients with glioblastoma with gross total resection were measured at three time points, 1 day following surgery, 4 weeks thereafter at the planning of RT and 5 weeks later (after 50 Gy was delivered) prior to boost planning. The differences between the surgical defect volumes were statistically significant ($p<0.001$), and based on the planning comparison, the authors concluded that the volume-adapted replanning during RT might reduce the irradiated volume of normal brain tissue and prevent a radiation target miss for boost RT (11). In line with this research, we detected relevant morphological changes on CT/MRI-based replanning performed prior to the boost irradiation. Moreover, patients were included with macroscopic tumors after partial resection and biopsy in which tumor response had contributed greatly to target volume changes in addition to post-surgical and RT-triggered reactions. In a preliminary study on three patients with GBM using integrated high-field MRI-LINAC, relevant volumetric changes in GBM tumor volume had been observed over the course of RT (47). Muruganandham et al. compared the status of tumor metabolic activity with MRI spectroscopy prior to and during the third week of RT, revealing a significant correlation with progression-free survival (PFS) (48). In our study, both the initial residual tumor volume and the extent of tumor shrinkage exhibited a significant impact on OS. The outcome of survival analysis showed no significant difference in terms of the initial size of the PTV. However, the GTV volume difference *i.e.* the difference between the GTV defined on the first plan and the tumorous mass seen on the replanning image, did show a significant correlation with OS in univariate analysis. Similarly, a relevant decrease in the size of the PTV (the PTV volume difference, analogous to the GTV volume difference) predicted better OS.

5.2. MRI-based image-guided adaptive brachytherapy for locally advanced cervical cancer in clinical routine: a single-institution experience

The studied IGABT technique based on multimodality imaging, modern radiobiology knowledge, and novel teletherapy and BT technologies is a rational approach but requires effort from the whole medical staff to adopt special skills and make a series of labor-intensive key steps in patient-management. For this new strategy, invaluable help is provided by the published protocol of the EMBRACE-II international clinical study (49). This book of precision on CRT and IGABT provides information on all challenges, including complex patient management, 3D image guidance, delineation and treatment planning, and proper BT applicator selection and arrangement. Furthermore, the EMBRACE team and Gyn GEC ESTRO collaborative group have been making efforts in the last two decades to disseminate the fundamentals of the aforementioned comprehensive concept through special training programs and within the frame of the ongoing EMBRACE-II international multi-center clinical study (50).

Due to the progression attributes of cervical carcinoma, sufficient loco-regional dose delivery is essential for tumor control. The review of Tanderup et al based on a large amount of clinical data demonstrated a strong correlation between the delivered dose to the target volumes and clinical outcome (51). The importance of dose escalation is also supported by the results of the EMBRACE-I study, achieving an excellent 5-year local control rate of 92% for the overall patient cohort (34). Meanwhile, the complete remission rate was 98%, and only 98/1,318 patients (7.4%) had local failure in the entire study population. Notably, 90% of these cases showed relapse within the BT target volume only. According to the report of Schmid et al, higher local failure rates were associated with the presence of tumor necrosis, uterine corpus or mesorectal space infiltration, or a larger initial tumor extent (CTVHR > 45 cm^3) (52). Moreover, an adenocarcinoma or adenosquamos carcinoma histology subtype was associated with a significantly higher risk of local failure. Delivering 85 Gy D90 dose to the CTVHR resulted in a 95% local control for squamous cell carcinomas vs. only 86% for adenocarcinoma/adenosquamous carcinoma cases at 3 years. In accordance with the retroEMBRACE data, overall treatment time (OTT) was also found to be an independent risk factor on clinical outcome (52). It is envisioned that the prospective follow-up data of EMBRACE-II will not only point to the role of radiation dose in improved outcome but will

demonstrate the feasibility of individually chosen dosing according to stage and tumor-related biomarkers in line with the importance of long-term quality of life (QOL) consideration (26). In other words, dose escalation and dose de-escalation will become individually chosen strategies in modern practice.

Our first series of patients and clinical data in this paper represent the efforts and learning period we went through during the integration of the modern IGART technique into our institutional practice. First, we systematically introduced the bladder protocol and rigid image fusion of the multiple series of treatment planning CT and diagnostic pelvic MRI and PET/CT scans for EBRT contouring, including the recommended complex volume of interest template, into the planning system. Accordingly, all patients received risk-adapted elective pelvic irradiation and SIB to pathological lymph nodes if applicable using IMRT planning aims; daily CBCT verification with correction to bony anatomy allowed for halving former PTV-CTV margins of 10 mm. Great attention was given to both teletherapy and chemotherapy as the basis of high-dose delivery at IGABT due to down-staging. Regarding the implementation of MRI-guided IGABT, the greatest challenges were ensuring the infrastructure of anesthesia, appropriate patient transport, adequate MRI imaging, and applicator reconstruction during the first couple of combined IC/IS treatment sessions. Handling the early target delineation and planning optimization uncertainties, we could gradually improve the BT target dose utilizing MRI guidance, resulting in a mean dose to the D90 CTVHR higher than 85 Gy. Although in the first few cases our main goal was to safely remain within the limits of OAR hard-dose constraints, later on we simultaneously aimed at the fulfillment of OAR soft-dose constraints and the planning aims of D90 CTVHR (90–95 Gy) and D98 GTVres (>95 Gy). The only explanation why the target dose was higher in the MRI-guided IGABT group could be that by having had identified the residual tumor and delivered a prespecified radiation dose to it, the dose to the CTVHR was unintentionally increased too. Our experience on eight cases (16,0%) having received BT with interstitial needles was favorable, indicating that the combined IC/IS technique is the adequate solution to serve this dual goal. The analysis in the retroEMBRACE study suggested that the simple IC BT technique has limitations in CTVHR dose coverage, especially in cases with larger residual tumor volumes (CTVHR > 30 cm^3), hence resulting in suboptimal local control (53). Another retroEMBRACE analysis by Fokdal et al. demonstrated that by using the combined IC/IS technique, the D90 CVTHR dose could be elevated by 9 Gy EQD_2 and consequently significantly higher local control rates were found in patients with

residual CTVHR > 30 cm^3 volumes without increasing toxicity as compared to the use of the sole IC BT technique (54). In fact, dedicated IC/IS applicators represent an excellent tool for the implementation of personalized treatment plans with unique complexity, allowing appropriate target coverage even if large residual tumors or parametrial infiltration are present (55, 56).

We have prospectively collected a set of acute toxicity measures possibly related to CRT; these were easily controlled and no serious side effects resulting in the cessation of therapy occurred. Due to the short follow-up time, the analysis of late toxicity is out of scope of this paper. Regarding long-term toxicity related to the described modern approach, the association between the delivered dose and the risk of moderate to severe chronic toxicity is highly supported by the results of the EMBRACE-I study. In terms of urinary morbidity, the dose to the bladder of $D2cm^3$ was correlated with the risk of grade 2 or higher fistula, cystitis, or bleeding; an increase of that dose from 75 Gy to 80 Gy almost doubled the risk of grade ≥2 cystitis (57). Beyond rectal and bowel $D2cm^3$ BT doses, the incidence of grade ≥2 diarrhea was associated with higher prescribed EBRT doses (45 vs. 50 Gy), total body V43 Gy values, and pathological lymph node SIB volumes (57). Attention to vaginal toxicity has recently come into view (58). Vaginal doses show extreme diversity depending on both the teletherapy and BT techniques. Vaginal dose de-escalation is crucial for the prevention of grade ≥2 vaginal stenosis; the EMBRACE-II protocol puts great emphasis on the documentation and control of the vaginal dose, assuming a maximum dose of 65 Gy EBRT + BT EQD2 to the ICRU recto-vaginal point. In addition, the doses to the mid and lower parts of the vagina must be assessed using the Posterior-Inferior Border of Symphysis (PIBS) dose points (59). It seems advantageous to use a ring and tandem applicator instead of a tandem and ovoids for this vaginal dose de-escalation approach (60). Interestingly, Mohamed et al. demonstrated that significant vaginal dose de-escalation may be achieved by reducing the dwell times in the ring or ovoids while increasing that in the tandem/interstitial needles without compromising the D90 CTVHR ≥85 Gy target dose (61).

Despite the excellent local control rates with the systematic utilization of IGART, with cases of advanced-stage disease, distant recurrence has still been a significant problem in light of the modest OS data. As a result, the need for progress has emerged recently in the field of novel systemic therapies. Currently, many clinical trials are ongoing using immunotherapy in addition to the standard CRT approach. Human papillomavirus (HPV)-associated cervical cancers are considered to be immunogenic tumors with increased neoantigen formation, high somatic

mutation rate, and enhanced programmed death-ligand 1 (PD-L1) expression (62, 63). Indeed, immunotherapy is now a part of standard care of metastatic/recurrent cervical carcinoma. Interestingly, the first phase III CALLA study failed to meet its primary endpoint when adding durvalumab to standard CRT in locoregional cervical carcinoma; PFS was not improved in the investigational arm (64). In contrast, the phase III ENGOT-cx11/KEYNOTE-A18 study - beyond PFS advantage - resulted in a significant increase in OS: at 3 years OS was 82.6% for pembrolizumab plus CRT vs 74.8% for CRT alone (65). Another approach, the use of induction chemotherapy prior to CRT, was tested in the phase III GCIG INTERLACE trial; a significant 9% PFS and 7% OS absolute benefit was demonstrated at 5 years of follow-up in favor of induction chemotherapy followed by CRT compared to standard CRT alone (66). The results of two later studies are encouraging and will probably exert a great impact on the standard of care of LACC in the near future. In addition, beyond traditional risk evaluation, the integration of biomarkers serving tailored management is awaited; notably, molecular biomarkers are being investigated in a Translational Research sub-study by EMBRACE as well (67).

The protocol used by us has been widely used within and outside of the EMBRACE network. In accordance with our modest experience, a report on a larger experience of 392 patients over 10 years has been published (68).

6. Summary and conclusion

6.1. Our findings support the great importance of monitoring anatomical changes in the course of fractionated postoperative brain tumor irradiation. A follow-up of the residual tumor during CRT and adaptation of the PTV to tumor volume changes result in increased accuracy of dose delivery to the tumor and relevant normal brain tissue sparing. According to our data, reduction of the PTV did not compromise survival; in contrast, it seemed to be beneficial. Our preliminary data on improved survival on the basis of a higher degree of PTV reduction warrant further clinical studies to confirm these encouraging results.

The implementation of an ART approach is suggested for postoperative irradiation of GBM to optimize coverage of the target and minimize the dose to OARs. The reported data confirm that significant changes occur in different brain structures and in the residual tumor during fractionated CRT. The tumor response and adapted boost volume definition exhibited a strong correlation to treatment outcome. Optimization of the imaging (MRI and amino acid-based PET/CT) for replanning could further improve the quality of the adaptive approach.

6.2. In the exploratory analysis of our first clinical experience, we found that the MRI-based IGABT technique is feasible and appropriate both for individual dose escalation and control of OAR doses and toxicities in the curative treatment of LACC patients. As a key element of modern IGART delivery this should be the preferred approach, especially in cases with large and/or irregular extent post-teletherapy residual tumors.

7. Novel findings

7.1. The institutional protocol for target volume delineation in high-grade gliomas was retrospectively validated.

7.2. A significant correlation was identified between postoperative RT parameter (GTV) and OS of patients.

7.3. Significant anatomical changes were observed in various brain structures and in the residual tumor during the course of fractionated CRT, as confirmed by repeated imaging.

7.4. A strong correlation was demonstrated between tumor response, the definition of the adapted boost volume, and treatment outcome, underscoring the clinical relevance of ART approach in high-grade gliomas.

7.5. In cervical cancer cases, repeated MRI-based adaptive planning prior and during BT has resulted in significant target volume dose escalation and allowed for optimal protection of adjacent OARs.

7.6. The real-world process of successfully implementing the highly demanding EMBRACE-II protocol for curative cervical cancer RT is presented, demonstrating continuous improvements over time in imaging quality, target delineation, adaptive planning strategies and target dose coverage.

8. Acknowledgements

First of all I am most grateful to my supervisor, Professor Katalin Hideghéty, whose encouragement and generous support helped me in the completion of this work.

I express my sincere gratitude to Professor Judit Oláh, director of the Department of Oncotherapy, University of Szeged, who provided excellent working conditions for me at the institute.

I am greatly indebted to Professor Zsuzsanna Kahán, former director of the department, Zoltán Varga, Ph.D. and Barbara Darázs Ph.D., whose invaluable support significantly contributed to my scientific work.

I am truly thankful for all the support and work of high standard provided by all the physicians, physicists and technician colleagues of the Department of Oncotherapy, University of Szeged that helped this dissertation to be born.

I am deeply grateful to my wife, family and parents for their unwavering support over the years.

9. References

1. Brock KK. Adaptive Radiotherapy: Moving Into the Future. *Semin Radiat Oncol*. 2019;29(3):181-184. doi:10.1016/j.semradonc.2019.02.011
2. Thibouw D, Truc G, Bertaut A, Chevalier C, Aubignac L, Mirjolet C. Clinical and dosimetric study of radiotherapy for glioblastoma: three-dimensional conformal radiotherapy versus intensity-modulated radiotherapy. *J Neurooncol*. 2018;137(2):429-438. doi:10.1007/s11060-017-2735-y
3. Briere TM, McAleer MF, Levy LB, Yang JN. Sparing of normal tissues with volumetric arc radiation therapy for glioblastoma: single institution clinical experience. *Radiat Oncol*. 2017;12(1):79. Published 2017 May 2. doi:10.1186/s13014-017-0810-3
4. Exeli AK, Kellner D, Exeli L, et al. Cerebral cortex dose sparing for glioblastoma patients: IMRT versus robust treatment planning. *Radiat Oncol*. 2018;13(1):20. Published 2018 Feb 6. doi:10.1186/s13014-018-0953-x
5. Petr J, Platzek I, Hofheinz F, et al. Photon vs. proton radiochemotherapy: Effects on brain tissue volume and perfusion. *Radiother Oncol*. 2018;128(1):121-127. doi:10.1016/j.radonc.2017.11.033
6. Mehta S, Gajjar SR, Padgett KR, et al. Daily Tracking of Glioblastoma Resection Cavity, Cerebral Edema, and Tumor Volume with MRI-Guided Radiation Therapy. *Cureus*. 2018;10(3):e2346. Published 2018 Mar 19. doi:10.7759/cureus.2346
7. Zhang L, Wang Z, Shi C, Long T, Xu XG. The impact of robustness of deformable image registration on contour propagation and dose accumulation for head and neck adaptive radiotherapy. *J Appl Clin Med Phys*. 2018;19(4):185-194. doi:10.1002/acm2.12361
8. Saito N, Schmitt D, Bangert M. Correlation between intrafractional motion and dosimetric changes for prostate IMRT: Comparison of different adaptive strategies. *J Appl Clin Med Phys*. 2018;19(4):87-97. doi:10.1002/acm2.12359
9. Matsuo Y. A promising result of locoregional tumor control with biologically adaptive radiotherapy in patients with locally advanced non-small cell lung cancer. *Transl Lung Cancer Res*. 2018;7(Suppl 2):S111-S113. doi:10.21037/tlcr.2018.03.01
10. Tsien C, Gomez-Hassan D, Ten Haken RK, et al. Evaluating changes in tumor volume using magnetic resonance imaging during the course of radiotherapy treatment of high-grade gliomas: Implications for conformal dose-escalation studies. *Int J Radiat Oncol Biol Phys*. 2005;62(2):328-332. doi:10.1016/j.ijrobp.2004.10.010

11. Kim TG, Lim DH. Interfractional variation of radiation target and adaptive radiotherapy for totally resected glioblastoma. *J Korean Med Sci*. 2013;28(8):1233-1237. doi:10.3346/jkms.2013.28.8.1233
12. Grossman R, Shimony N, Shir D, et al. Dynamics of FLAIR Volume Changes in Glioblastoma and Prediction of Survival. *Ann Surg Oncol*. 2017;24(3):794-800. doi:10.1245/s10434-016-5635-z
13. Champ CE, Siglin J, Mishra MV, et al. Evaluating changes in radiation treatment volumes from post-operative to same-day planning MRI in High-grade gliomas. *Radiat Oncol*. 2012;7:220. Published 2012 Dec 21. doi:10.1186/1748-717X-7-220
14. Liang HT, Chen WY, Lai SF, et al. The extent of edema and tumor synchronous invasion into the subventricular zone and corpus callosum classify outcomes and radiotherapy strategies of glioblastomas. *Radiother Oncol*. 2017;125(2):248-257. doi:10.1016/j.radonc.2017.09.024
15. Chatterjee A, Serban M, Abdulkarim B, et al. Performance of Knowledge-Based Radiation Therapy Planning for the Glioblastoma Disease Site. *Int J Radiat Oncol Biol Phys*. 2017;99(4):1021-1028. doi:10.1016/j.ijrobp.2017.07.012
16. Hofmaier J, Kantz S, Söhn M, et al. Hippocampal sparing radiotherapy for glioblastoma patients: a planning study using volumetric modulated arc therapy. *Radiat Oncol*. 2016;11(1):118. Published 2016 Sep 8. doi:10.1186/s13014-016-0695-6
17. Mann J, Ramakrishna R, Magge R, Wernicke AG. Advances in Radiotherapy for Glioblastoma. *Front Neurol*. 2018;8:748. Published 2018 Jan 15. doi:10.3389/fneur.2017.00748
18. Niyazi M, Geisler J, Siefert A, et al. FET-PET for malignant glioma treatment planning. *Radiother Oncol*. 2011;99(1):44-48. doi:10.1016/j.radonc.2011.03.001
19. Ghose A, Lim G, Husain S. Treatment for glioblastoma multiforme: current guidelines and Canadian practice. *Curr Oncol*. 2010;17(6):52-58. doi:10.3747/co.v17i6.574
20. Tsien C, Moughan J, Michalski JM, et al. Phase I three-dimensional conformal radiation dose escalation study in newly diagnosed glioblastoma: Radiation Therapy Oncology Group Trial 98-03. *Int J Radiat Oncol Biol Phys*. 2009;73(3):699-708. doi:10.1016/j.ijrobp.2008.05.034
21. Niyazi M, Andratschke N, Bendszus M, et al. ESTRO-EANO guideline on target delineation and radiotherapy details for glioblastoma. *Radiother Oncol*. 2023;184:109663. doi:10.1016/j.radonc.2023.109663

22. Cabrera AR, Kirkpatrick JP, Fiveash JB, et al. Radiation therapy for glioblastoma: Executive summary of an American Society for Radiation Oncology Evidence-Based Clinical Practice Guideline. *Pract Radiat Oncol*. 2016;6(4):217-225. doi:10.1016/j.prro.2016.03.007
23. Niyazi M, Brada M, Chalmers AJ, et al. ESTRO-ACROP guideline "target delineation of glioblastomas". *Radiother Oncol*. 2016;118(1):35-42. doi:10.1016/j.radonc.2015.12.003
24. Kruser TJ, Bosch WR, Badiyan SN, et al. NRG brain tumor specialists consensus guidelines for glioblastoma contouring. *J Neurooncol*. 2019;143(1):157-166. doi:10.1007/s11060-019-03152-9
25. Krasznai Z, Molnár S. A méhnyakrák epidemiológiája Magyarországon és a világban [Epidemiology of cervical cancer in Hungary and the world]. *Magy Onkol*. 2022;66(4):262-269.
26. Pötter R, Tanderup K, Kirisits C, et al. The EMBRACE II study: The outcome and prospect of two decades of evolution within the GEC-ESTRO GYN working group and the EMBRACE studies. *Clin Transl Radiat Oncol*. 2018;9:48-60. Published 2018 Jan 11. doi:10.1016/j.ctro.2018.01.001
27. Landoni F, Maneo A, Colombo A, et al. Randomised study of radical surgery versus radiotherapy for stage Ib-IIa cervical cancer. *Lancet*. 1997;350(9077):535-540. doi:10.1016/S0140-6736(97)02250-2
28. Whitney CW, Sause W, Bundy BN, et al. Randomized comparison of fluorouracil plus cisplatin versus hydroxyurea as an adjunct to radiation therapy in stage IIB-IVA carcinoma of the cervix with negative para-aortic lymph nodes: a Gynecologic Oncology Group and Southwest Oncology Group study. *J Clin Oncol*. 1999;17(5):1339-1348. doi:10.1200/JCO.1999.17.5.1339
29. Morris M, Eifel PJ, Lu J, et al. Pelvic radiation with concurrent chemotherapy compared with pelvic and para-aortic radiation for high-risk cervical cancer. *N Engl J Med*. 1999;340(15):1137-1143. doi:10.1056/NEJM199904153401501
30. Rose PG, Bundy BN, Watkins EB, et al. Concurrent cisplatin-based radiotherapy and chemotherapy for locally advanced cervical cancer. *N Engl J Med*. 1999;340(15):1144-1153. doi:10.1056/NEJM199904153401502
31. Keys HM, Bundy BN, Stehman FB, et al. Cisplatin, radiation, and adjuvant hysterectomy compared with radiation and adjuvant hysterectomy for bulky stage IB cervical carcinoma. *N Engl J Med*. 1999;340(15):1154-1161. doi:10.1056/NEJM199904153401503

32. Peters WA 3rd, Liu PY, Barrett RJ 2nd, et al. Concurrent chemotherapy and pelvic radiation therapy compared with pelvic radiation therapy alone as adjuvant therapy after radical surgery in high-risk early-stage cancer of the cervix. *J Clin Oncol*. 2000;18(8):1606-1613. doi:10.1200/JCO.2000.18.8.1606
33. Chargari C, Renard S, Espenel S, et al. Can stereotactic body radiotherapy replace brachytherapy for locally advanced cervical cancer? French society for radiation oncology statement. *Cancer Radiother*. 2020;24(6-7):706-713. doi:10.1016/j.canrad.2020.05.003
34. Pötter R, Tanderup K, Schmid MP, et al. MRI-guided adaptive brachytherapy in locally advanced cervical cancer (EMBRACE-I): a multicentre prospective cohort study. *Lancet Oncol*. 2021;22(4):538-547. doi:10.1016/S1470-2045(20)30753-1
35. Sturdza A, Pötter R, Fokdal LU, et al. Image guided brachytherapy in locally advanced cervical cancer: Improved pelvic control and survival in RetroEMBRACE, a multicenter cohort study. *Radiother Oncol*. 2016;120(3):428-433. doi:10.1016/j.radonc.2016.03.011
36. Pötter R, Haie-Meder C, Van Limbergen E, et al. Recommendations from gynaecological (GYN) GEC ESTRO working group (II): concepts and terms in 3D image-based treatment planning in cervix cancer brachytherapy-3D dose volume parameters and aspects of 3D image-based anatomy, radiation physics, radiobiology. *Radiother Oncol*. 2006;78(1):67-77. doi:10.1016/j.radonc.2005.11.014
37. Tan Mbbs Mrcp Frcr Md LT, Tanderup PhD K, Kirisits PhD C, et al. Image-guided Adaptive Radiotherapy in Cervical Cancer. *Semin Radiat Oncol*. 2019;29(3):284-298. doi:10.1016/j.semradonc.2019.02.010
38. Dimopoulos JC, Petrow P, Tanderup K, et al. Recommendations from Gynaecological (GYN) GEC-ESTRO Working Group (IV): Basic principles and parameters for MR imaging within the frame of image based adaptive cervix cancer brachytherapy. *Radiother Oncol*. 2012;103(1):113-122. doi:10.1016/j.radonc.2011.12.024
39. ICRU REPORT 89: Prescribing, Recording, and Reporting Brachytherapy for Cancer of the Cervix. *J ICRU*. 2013;13(1-2):. doi:10.1093/jicru/ndw027
40. Darázs B, Ruskó L, Végváry Z, et al. Subventricular zone volumetric and dosimetric changes during postoperative brain tumor irradiation and its impact on overall survival. *Phys Med*. 2019;68:35-40. doi:10.1016/j.ejmp.2019.10.039
41. Ho KF, Marchant T, Moore C, et al. Monitoring dosimetric impact of weight loss with kilovoltage (kV) cone beam CT (CBCT) during parotid-sparing IMRT and concurrent chemotherapy. *Int J Radiat Oncol Biol Phys*. 2012;82(3):e375-e382. doi:10.1016/j.ijrobp.2011.07.004

42. Brouwer CL, Steenbakkers RJ, Langendijk JA, Sijtsema NM. Identifying patients who may benefit from adaptive radiotherapy: Does the literature on anatomic and dosimetric changes in head and neck organs at risk during radiotherapy provide information to help?. *Radiother Oncol*. 2015;115(3):285-294. doi:10.1016/j.radonc.2015.05.018
43. Lim-Reinders S, Keller BM, Al-Ward S, Sahgal A, Kim A. Online Adaptive Radiation Therapy. *Int J Radiat Oncol Biol Phys*. 2017;99(4):994-1003. doi:10.1016/j.ijrobp.2017.04.023
44. Robar JL, Day A, Clancey J, et al. Spatial and dosimetric variability of organs at risk in head-and-neck intensity-modulated radiotherapy. *Int J Radiat Oncol Biol Phys*. 2007;68(4):1121-1130. doi:10.1016/j.ijrobp.2007.01.030
45. Marzi S, Pinnarò P, D'Alessio D, et al. Anatomical and dose changes of gross tumour volume and parotid glands for head and neck cancer patients during intensity-modulated radiotherapy: effect on the probability of xerostomia incidence. *Clin Oncol (R Coll Radiol)*. 2012;24(3):e54-e62. doi:10.1016/j.clon.2011.11.006
46. Surucu M, Shah KK, Roeske JC, Choi M, Small W Jr, Emami B. Adaptive Radiotherapy for Head and Neck Cancer. *Technol Cancer Res Treat*. 2017;16(2):218-223. doi:10.1177/1533034616662165
47. Ruschin ME, Sahgal A, Chugh B, et al. Preliminary investigation of adaptive glioblastoma radiation therapy using the integrated high-field MRI-LINAC. Int J Radiat Oncol Biol Phys 99(2): 717, 2017
48. Muruganandham M, Clerkin PP, Smith BJ, et al. 3-Dimensional magnetic resonance spectroscopic imaging at 3 Tesla for early response assessment of glioblastoma patients during external beam radiation therapy. *Int J Radiat Oncol Biol Phys*. 2014;90(1):181-189. doi:10.1016/j.ijrobp.2014.05.014
49. EMBRACE II protocol version 1.0 Available online: https://www.embracestudy.dk/UserUpload/PublicDocuments/EMBRACE%20II%20Protocol.pdf
50. Tan LT, Tanderup K, Kirisits C, et al. Education and training for image-guided adaptive brachytherapy for cervix cancer - The (GEC)-ESTRO/EMBRACE perspective. *Brachytherapy*. 2020;19(6):827-836. doi:10.1016/j.brachy.2020.06.012
51. Tanderup K, Nesvacil N, Kirchheiner K, et al. Evidence-Based Dose Planning Aims and Dose Prescription in Image-Guided Brachytherapy Combined With Radiochemotherapy in Locally Advanced Cervical Cancer. *Semin Radiat Oncol*. 2020;30(4):311-327. doi:10.1016/j.semradonc.2020.05.008

52. Schmid MP, Lindegaard JC, Mahantshetty U, et al. Risk Factors for Local Failure Following Chemoradiation and Magnetic Resonance Image-Guided Brachytherapy in Locally Advanced Cervical Cancer: Results From the EMBRACE-I Study. *J Clin Oncol*. 2023;41(10):1933-1942. doi:10.1200/JCO.22.01096
53. Tanderup K, Fokdal LU, Sturdza A, et al. Effect of tumor dose, volume and overall treatment time on local control after radiochemotherapy including MRI guided brachytherapy of locally advanced cervical cancer. *Radiother Oncol*. 2016;120(3):441-446. doi:10.1016/j.radonc.2016.05.014
54. Fokdal L, Sturdza A, Mazeron R, et al. Image guided adaptive brachytherapy with combined intracavitary and interstitial technique improves the therapeutic ratio in locally advanced cervical cancer: Analysis from the retroEMBRACE study. *Radiother Oncol*. 2016;120(3):434-440. doi:10.1016/j.radonc.2016.03.020
55. Dimopoulos JC, Kirisits C, Petric P, et al. The Vienna applicator for combined intracavitary and interstitial brachytherapy of cervical cancer: clinical feasibility and preliminary results. *Int J Radiat Oncol Biol Phys*. 2006;66(1):83-90. doi:10.1016/j.ijrobp.2006.04.041
56. Mahantshetty U, Sturdza A, Naga Ch P, et al. Vienna-II ring applicator for distal parametrial/pelvic wall disease in cervical cancer brachytherapy: An experience from two institutions: Clinical feasibility and outcome. *Radiother Oncol*. 2019;141:123-129. doi:10.1016/j.radonc.2019.08.004
57. Spampinato S, Fokdal LU, Pötter R, et al. Risk factors and dose-effects for bladder fistula, bleeding and cystitis after radiotherapy with imaged-guided adaptive brachytherapy for cervical cancer: An EMBRACE analysis. *Radiother Oncol*. 2021;158:312-320. doi:10.1016/j.radonc.2021.01.019
58. Serban M, de Leeuw AAC, Tanderup K, Jürgenliemk-Schulz IM. Vaginal dose-surface maps in cervical cancer brachytherapy: Methodology and preliminary results on correlation with morbidity. *Brachytherapy*. 2021;20(3):565-575. doi:10.1016/j.brachy.2021.02.004
59. Westerveld H, Pötter R, Berger D, et al. Vaginal dose point reporting in cervical cancer patients treated with combined 2D/3D external beam radiotherapy and 2D/3D brachytherapy. *Radiother Oncol*. 2013;107(1):99-105. doi:10.1016/j.radonc.2013.04.009
60. Westerveld H, Kirchheiner K, Nout RA, et al. Dose-effect relationship between vaginal dose points and vaginal stenosis in cervical cancer: An EMBRACE-I sub-study. *Radiother Oncol*. 2022;168:8-15. doi:10.1016/j.radonc.2021.12.034

61. Mohamed S, Lindegaard JC, de Leeuw AA, et al. Vaginal dose de-escalation in image guided adaptive brachytherapy for locally advanced cervical cancer. *Radiother Oncol*. 2016;120(3):480-485. doi:10.1016/j.radonc.2016.05.020
62. Faye MD, Alfieri J. Advances in Radiation Oncology for the Treatment of Cervical Cancer. *Curr Oncol*. 2022;29(2):928-944. Published 2022 Feb 9. doi:10.3390/curroncol29020079
63. Mezache L, Paniccia B, Nyinawabera A, Nuovo GJ. Enhanced expression of PD L1 in cervical intraepithelial neoplasia and cervical cancers. *Mod Pathol*. 2015;28(12):1594-1602. doi:10.1038/modpathol.2015.108
64. Monk BJ, Toita T, Wu X, et al. Durvalumab versus placebo with chemoradiotherapy for locally advanced cervical cancer (CALLA): a randomised, double-blind, phase 3 trial. *Lancet Oncol*. 2023;24(12):1334-1348. doi:10.1016/S1470-2045(23)00479-5
65. Lorusso D, Xiang Y, Hasegawa K, et al. Pembrolizumab or placebo with chemoradiotherapy followed by pembrolizumab or placebo for newly diagnosed, high-risk, locally advanced cervical cancer (ENGOT-cx11/GOG-3047/KEYNOTE-A18): a randomised, double-blind, phase 3 clinical trial. *Lancet*. 2024;403(10434):1341-1350. doi:10.1016/S0140-6736(24)00317-9
66. McCormack M, Eminowicz G, Gallardo D, et al. Induction chemotherapy followed by standard chemoradiotherapy versus standard chemoradiotherapy alone in patients with locally advanced cervical cancer (GCIG INTERLACE): an international, multicentre, randomised phase 3 trial. *Lancet*. 2024;404(10462):1525-1535. doi:10.1016/S0140-6736(24)01438-7
67. EMBRACE: https://www.embracestudy.dk/
68. Chimeno J, Fuentemilla N, Monasor P, et al. Evaluation of the impact of EMBRACE II protocol in Spanish centers, with a large cohort of patients using a ranking index. *J Contemp Brachytherapy*. 2021;13(6):680-686. doi:10.5114/jcb.2021.112119

10. Appendix